Compensation of Systematic Errors in ZUPT-Aided Pedestrian Inertial Navigation

Yusheng Wang, Yu-Wei Lin, Sina Askari, Chi-Shih Jao, and Andrei M. Shkel
MicroSystems Laboratory, University of California, Irvine, CA, USA
Email: {yushengw, yuweil4, askaris, chishihj, andrei.shkel}@uci.edu

***Abstract*—We present a method to identify and compensate systematic errors in the ZUPT-aided pedestrian inertial navigation. We considered two main categories of systematic errors resulting in an underestimate of the length of the trajectory and a drift in the heading of the trajectory. In this study, we identified the dominant factors resulting in the trajectory length and heading errors to be residual velocity during the stance phase and g-sensitivity error of the gyroscopes, respectively. Magnetic motion tracking system was used to record the velocity of the foot during the stance phase. Rate table, tilt table, and shaker were used to calibrate the IMU g-sensitivity. After compensation, a more than $6\times$ systematic error reduction was demonstrated from 3.24m to 0.50m during a 100m straight line trajectory. To the best of our knowledge, this study is the first attempt to reduce the systematic errors in the ZUPT-aided pedestrian inertial navigation algorithmically, without adding extra sensing modalities.**

***Index Terms*—Pedestrian navigation, ZUPT, systematic errors, g-sensitivity, stance phase.**

I. Introduction

In the past twenty years, pedestrian inertial navigation has been made possible by the development of MEMS-based Inertial Measurement Units (IMU), due to their small sizes, low costs, and continuously improving performances [1]. However, using classical inertial navigation algorithms without applying aiding techniques, the navigation error will reach 1m within a few seconds of navigation with a typical consumer-grade IMU, or within 20 seconds with tactical-grade IMUs. Zero-Velocity Update (ZUPT) - aided navigation algorithm is one of the commonly used techniques to compensate for navigation errors in pedestrian inertial navigation [2]. It takes advantage of stationary state of the foot during the stance phases to limit the propagation of navigation errors. It has been demonstrated that ZUPT-aided navigation algorithm can greatly reduce navigation errors by bounding the error in velocity estimate [3].

Two phenomena have been observed that limit the extent of navigation accuracy improvement: underestimate of the length of the trajectory and systematic drift of the orientation of the trajectory. It has been demonstrated that systematic errors can be on the same order, or even larger than errors caused by IMU noise [4]. Therefore, further improvement of the navigation accuracy in the ZUPT-aided pedestrian inertial navigation requires identification of error sources and compensation of systematic errors.

There are two major categories of error sources that contribute to systematic errors in ZUPT-aided pedestrian inertial navigation. One category is related to the aiding algorithm. Extended Kalman Filter (EKF) is needed to incorporate ZUPT information to the inertial navigation, where an uncorrelated and white noise is assumed. However, it has been shown that the innovations in the EKF are self-correlated [5]. Besides, the velocity of the foot has been shown to be not exactly zero during the stance phase [6]. Therefore, the pseudo-measurement of zero-velocity of the foot is likely to introduce extra errors. The other category of errors is related to dynamics that IMUs experience during the gait cycle. For example, accelerations as high as $15g$ and angular rates as high as $1500°/s$ can be achieved during running [7]. The high acceleration may lead to a large g-sensitivity and g-square sensitivity errors of the gyroscopes [8]. The fast changes of the specific force during the heel strike may also induce IMU errors, if the IMU bandwidth is not large enough [5]. This category of errors is not related to ZUPT implementation and is present in any strapdown inertial navigation.

Attempts to solve the issues in the ZUPT-aided pedestrian inertial navigation have been conducted in the past ten years. It was proposed in [9] to add coefficients of the gyroscope g-sensitivity errors in the EKF, and a reduction of navigation errors of about 50% was demonstrated. However, due to a limited observability of the yaw angle error, which is one of the major error sources in the ZUPT-aided pedestrian inertial navigation [10], EKF cannot fully estimate the gyroscope errors, especially along the z-axis. As a result, only a moderate improvement was shown. To improve the yaw angle observability, different sensing modalities have been proposed, such as magnetometry [11] and directional ranging [12], but including extra sensing modalities will increase the cost and complexity of the navigation system. For indoor pedestrian navigation, the knowledge of changes in orientation within a building structure was proposed to be used to compensate for yaw angle drift [13], but this approach requires a predefined knowledge of the environment, and is not considered as self-contained navigation. It was proposed in [14] to mount IMUs on both feet, and couple the results from the two IMUs by limiting the distance between them, such that the systematic errors from the two IMUs on two feet can be canceled. However, the systematic errors of the two feet may

This work was performed under the following financial assistance award: 70NANB17H192 from U.S. Department of Commerce, National Institute of Standards and Technology (NIST).

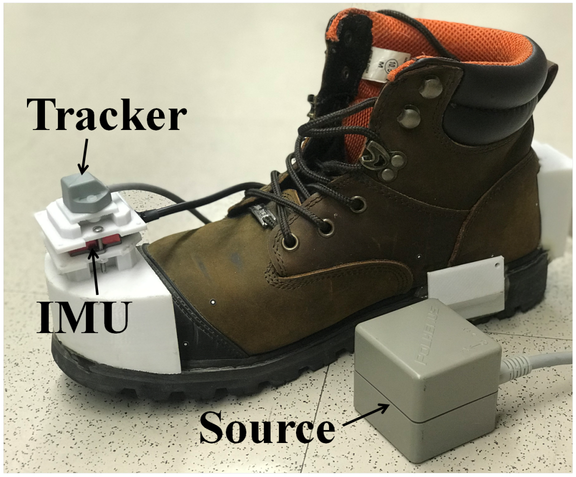

Fig. 1. Experimental setup to record the motion of the foot during the stance phase.

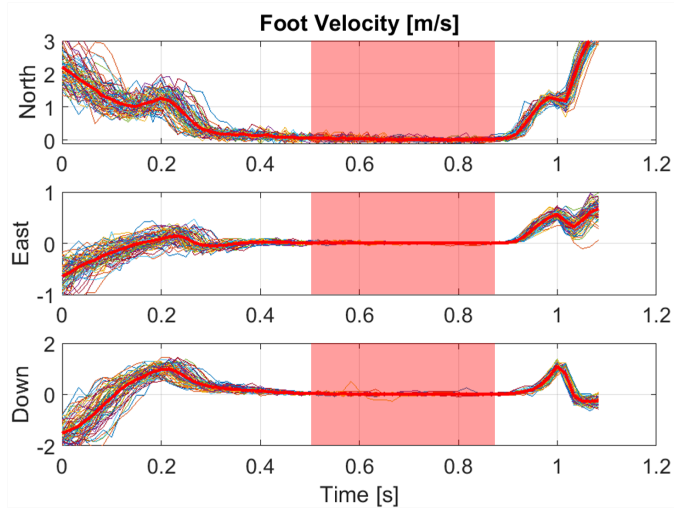

Fig. 2. Velocity of the foot along three directions during a gait cycle. The red solid lines are the averaged velocity along three directions.

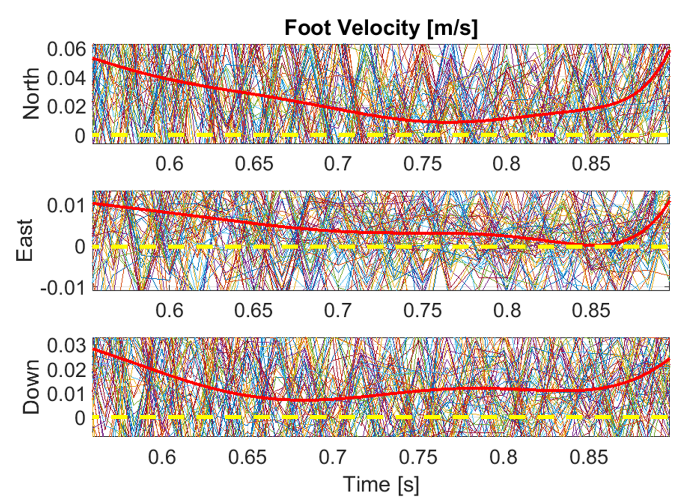

Fig. 3. Zoomed-in view of the velocity of the foot during the stance phase. The yellow dashed lines correspond to zero-velocity state.

be asymmetric due to asymmetric gait patterns of the two feet, thus the algorithm may not be generally feasible. All these previous studies did not identify the source of systematic errors in the ZUPT-aided pedestrian inertial navigation. In this study, we intend to fill the gap in previous studies, identify the major sources of the systematic errors, and then propose an approach to compensate them in the navigation algorithm.

II. Error Source Analysis

Two major errors in the ZUPT-aided pedestrian inertial navigation are underestimate of the length of the trajectory and systematic drift of orientation of the trajectory. In this section, we identify the error sources in the pedestrian navigation.

A. Trajectory Length Underestimate

It has been demonstrated that underestimate of the trajectory length is related to the zero-velocity assumption of the foot during the stance phase [5]. An excessive use of the ZUPT may deteriorate the estimation results, and may introduce errors as high as 15% of the total length of the trajectory [7].

To quantitatively analyze the relation between the ZUPT assumption and underestimate of the trajectory length, the motion of the foot during the stance phase needs to be recorded and analyzed. A magnetic motion tracking system (Polhemus PATRIOT) was used in this study. There are two parts in the system: the magnetic source was placed on the floor as a reference, and the tracker was mounted by a custom fixture on top of the IMU (VectorNav VN-200). The experimental setup is shown in Fig. 1. The tracking system was able to track the relative position and orientation between the tracker and the source with a resolution of $1mm$ and $0.1°$ and a sampling frequency of $60Hz$ [15]. Velocity of the foot was derived by taking derivative of the relative position with respect to time.

70 gait cycles were recorded with a walking pace of approximately 84 steps per minute toward the North, and the results are shown in Fig. 2. The red solid lines are the averaged velocity along three directions. Stance phase approximately corresponds to the time period between 0.5s and 0.9s (indicated by the red box), and the velocity of the foot is close to zero during the stance phase. However, Fig. 3 shows the zoomed-in view of the velocity during the stance phase. Residual velocity on the order of $0.01m/s$ are clearly observed. Assuming the non-zero residual velocity during the stance phase to be zero would introduce a systematic error.

Underestimate of the trajectory length is directly related to the residual velocity during the stance phase. However, the residual velocity is not constant during the stance phase. Therefore, its average value is related to the length of the stance phase as determined by the ZUPT detector. One of the most commonly used ZUPT detectors is Stance Hypothesis Optimal dEtection (SHOE) [16]. Based on Generalized Likelihood Ratio Test (GLRT), SHOE extracts a test statistic based on readouts, both from accelerometers and gyroscopes of the IMU, and compares it with a pre-defined threshold. The stance

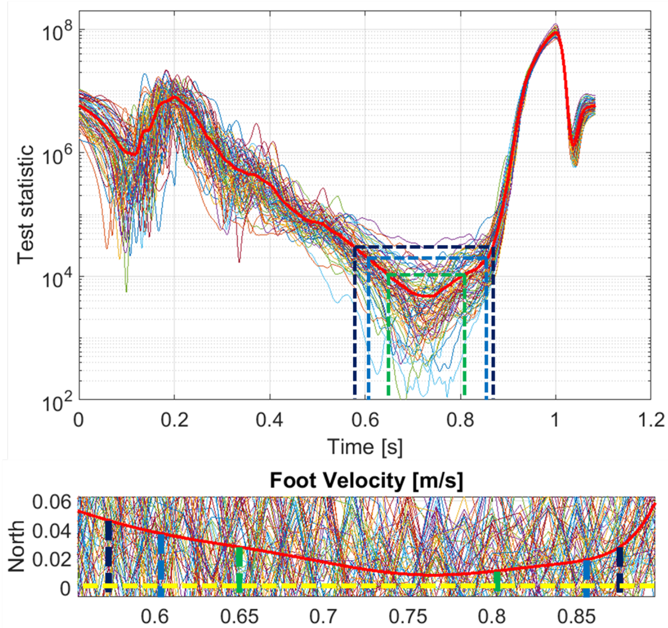

Fig. 4. The upper figure shows the test statistics of the same 70 steps recorded previously. Red solid line is the averaged value. The lower figure shows the residual velocity of the foot along the trajectory during the stance phase. The green, light blue, and dark blue dash lines correspond to threshold levels of 1×10^4, 2×10^4, and 3×10^4, respectively.

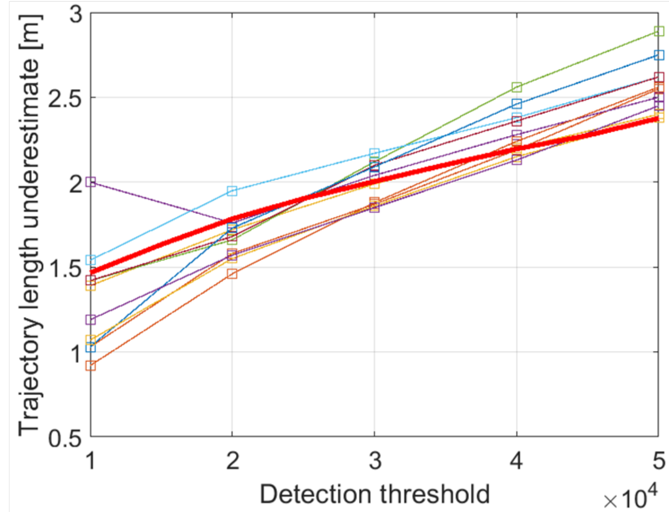

Fig. 5. Relation between the underestimate of trajectory length and the ZUPT detection threshold. The red solid line is the result from the previous analysis and the thinner lines are experimental results from 10 different runs.

phase is detected if the test statistic is lower than the threshold. Fig. 4 shows the test statistics of the same 70 steps recorded previously, and the red solid line is the averaged value.

The level of test statistic is not a constant even when the foot is in the stance phase. Therefore, the length of the detected stance phase is related to the value of the pre-defined threshold. For example, the detected stance phase is between 0.65s and 0.8s if the threshold is set to 1×10^4 (the dashed green line in Fig. 4). If the threshold is increased to 3×10^4, the detected stance phase is between 0.57s and 0.86s (the dashed dark blue line in Fig. 4). A longer detected stance phase leads to a higher averaged residual velocity of the foot during the stance phase, and therefore a higher systematic error will be introduced.

To experimentally verify the effects of residual velocity during the stance phase, IMU data were recorded for ten straight trajectories with length of 100m. The walking pace was 84 steps per minute. For each of the trajectory, thresholds ranging from 1×10^4 to 5×10^4 were applied in the ZUPT detector, and the underestimate of the trajectory length was recorded and shown in Fig. 5. The red solid line is the result from the previous analysis and the thinner lines are experimental results. A good match was demonstrated, verifying that the residual velocity during the stance phase is the major factor that leads to the underestimate of the trajectory length.

B. Trajectory Orientation Drift

Trajectory orientation drift in the ZUPT-aided pedestrian inertial navigation is believed to be related to the g-sensitivity of gyroscopes [9], [17]. Due to a severe dynamics of the foot during walking, the heading angle error was demonstrated to accumulate at a rate of $135°/h$, even though the gyroscope bias instability was only $3°/h$ [18].

To relate the trajectory orientation drift and the heading angle drift, IMU data were recorded for a straight line trajectory of 550m toward the North. The experimentally recorded trajectory is shown by the blue solid line in Fig. 6, showing a drift to the right. The estimated heading angle is shown in the inset in Fig. 6, showing a drift at the rate of $0.028°/s$. The red dashed line shows an analytically generated trajectory assuming a constant speed and a heading angle increase at the rate of $0.028°/s$. The experimental and generated trajectories match each other with a difference within 5m, indicating that the heading angle drift is the major factor that leads to the trajectory orientation drift.

To understand the reason for the heading angle drift, we fully calibrated the IMU to obtain not only gyroscope and accelerometer biases, but also misalignment and gyroscope g-sensitivity. During calibration, the IMU was rigidly mounted on a tilt table to achieve different orientations, and the tilt table was mounted on a single-axis rate table (IDEAL AEROSMITH 1270VS) to generate a constant rotation. The experimental setup is shown in Fig. 7 (a). A standard IMU calibration procedure was followed [19], and the calibration results are as follows:

$$b_a = \begin{bmatrix} -0.025 \\ -0.0176 \\ 0.1955 \end{bmatrix}, M_a = \begin{bmatrix} 1.0020 & -0.0083 & -0.0042 \\ 0.0055 & 0.9986 & 0.0051 \\ 0.0067 & -0.0039 & 0.9964 \end{bmatrix},$$

$$b_g = \begin{bmatrix} -0.0893 \\ 0.0375 \\ -0.0412 \end{bmatrix}, M_g = \begin{bmatrix} 0.9972 & -0.0041 & -0.0067 \\ 0.0041 & 0.9972 & 0.0052 \\ 0.0067 & -0.0027 & 1.0019 \end{bmatrix},$$

$$G_g = \begin{bmatrix} 0.0041 & 0.0002 & -0.0005 \\ 0.0002 & 0.0025 & 0.0002 \\ -0.0005 & -0.0006 & -0.0022 \end{bmatrix}.$$

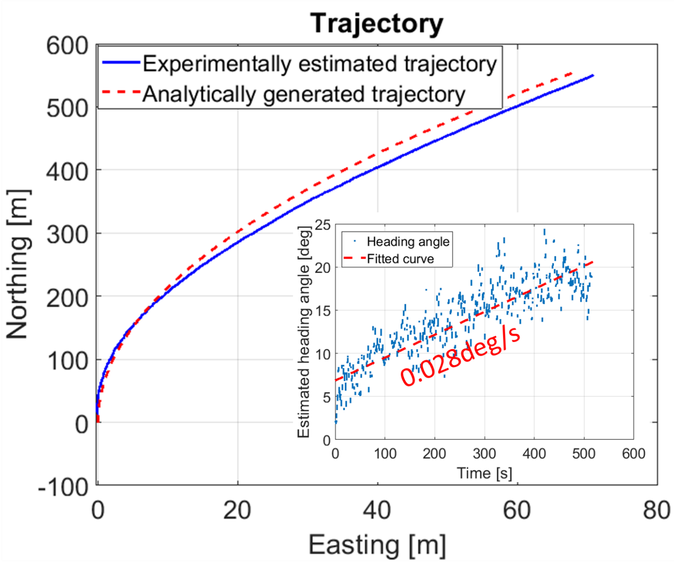

Fig. 6. The blue solid line is an estimated trajectory, and the red dashed line is an analytically generated trajectory with heading angle increase at a rate of $0.028°/s$. Note that the scales for x and y axes are different. The inset shows that the estimated heading angle increases at a rate of $0.028°/s$.

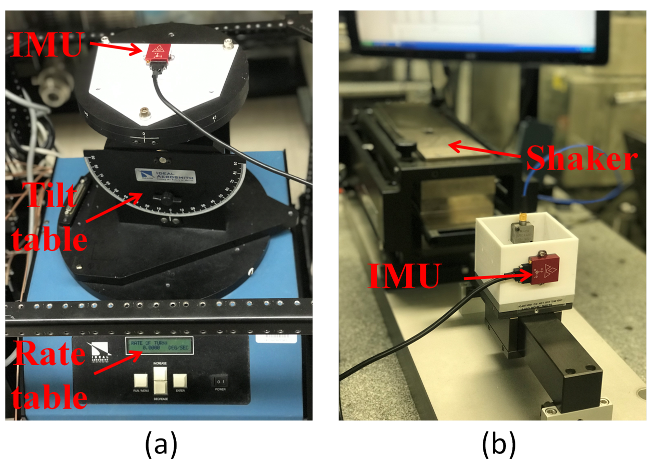

Fig. 7. (a) Experimental setup to statically calibrate IMU; (b) experimental setup to measure the relation between gyroscope g-sensitivity and acceleration frequency.

where b_a is the accelerometer bias in m/s^2, b_g is the gyroscope bias in $°/s$, M_a is the accelerometer misalignment matrix, M_g is the gyroscope misalignment matrix, and G_g is the gyroscope g-sensitivity matrix in $°/s/(m/s^2)$. These values were used in the IMU readout compensation before fed into the navigation algorithm. Note that the g-sensitivity of the gyroscope is on the order of $0.002°/s/(m/s^2)$. A shock on the order of $10g$, which is typical for a foot-mounted IMU, would cause a gyroscope bias of $0.2°/s$ and result in a large navigation error, if not compensated.

Note that g-sensitivity of gyroscopes was obtained in a static condition. Since the IMU will experience severe dynamics during navigation, a measurement of the gyroscope g-sensitivity in dynamic conditions was also necessary. To achieve it, the

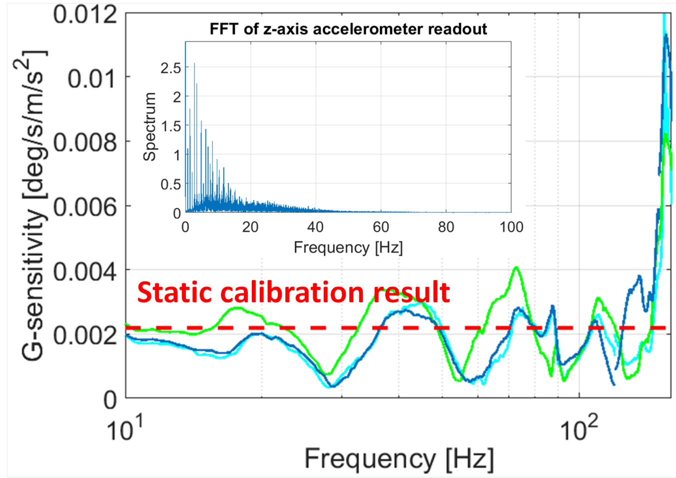

Fig. 8. Relation between the gyroscope g-sensitivity and the vibration frequency obtained from 3 independent measurements. The red dashed line is the gyroscope g-sensitivity measured in static calibration. Inset is the FFT of the z-axis accelerometer readout during a typical walking of $2min$.

IMU was rigidly mounted on a shaker (APS Dynamics APS-500), and the gyroscope readouts were recorded while the shaker generated vibration with different frequencies, ranging from 10Hz to 160Hz. Three independent measurements were conducted to guarantee repeatability. A relation between the gyroscope g-sensitivity and the vibration frequency is shown in Fig. 8. Gyroscope g-sensitivity is shown to remain relatively stable around $0.0022°/s/(m/s^2)$ until the vibration frequency is above 140Hz. Inset is the Fast Fourier Transform (FFT) of the z-axis accelerometer readout during a typical walking of $2min$, and the spectrum dies out with frequencies higher than 80Hz. Therefore, the gyroscope g-sensitivity can be considered constant for the whole frequency range in the case of pedestrian navigation.

III. Error Compensation Results

Two steps were taken to compensate for systematic errors identified in this paper: (1) calibrate the IMU readouts to remove the effects of sensor biases, misalignment, and especially gyroscope g-sensitivity; (2) set the pseudo-measurement of the velocity of the foot during the stance phase according to the gait pattern and ZUPT threshold instead of zero.

Experiments were conducted to verify the effects of compensation. The IMU was mounted on top of the toes. A straight line trajectory of $99.6m$ was used and 40 sets of data were recorded in total. The navigation results with and without compensation are shown in Fig. 9. It can be seen that the drift in trajectory orientation has been compensated, while the compensation effects along the trajectory cannot be seen clearly due to the scale. Fig. 10 shows the ending points of the 40 trajectories with and without compensation. The dashed lines are the 3σ boundaries of the results. Note that they are approximately of the same size, since they are mainly related to the IMU noise, which is not compensated in this study. The averaged navigation error perpendicular

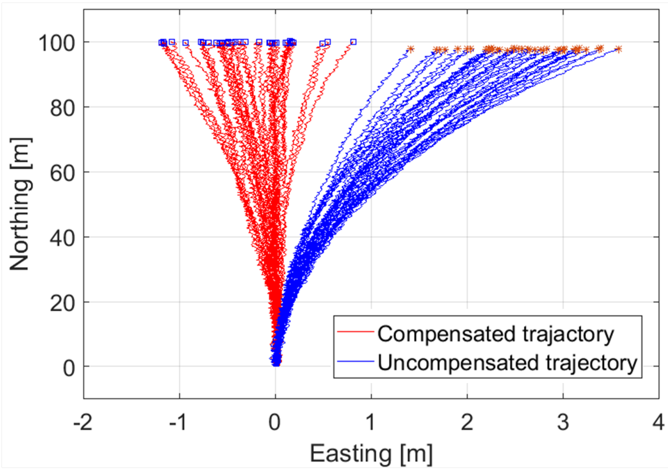

Fig. 9. Comparison of trajectories with and without systematic error compensation. Note that the scales for x and y axes are different.

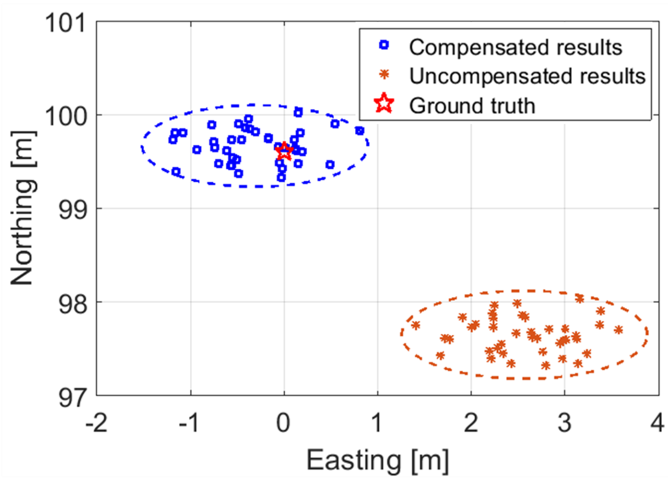

Fig. 10. Comparison of the ending points with and without systematic error compensation. The dashed lines are the 3σ boundaries of the results.

to the trajectory for 40 runs was $2.57m$ and the averaged underestimate of the length of the trajectory was $1.95m$ before compensation. After compensation, the error was reduced to $0.31m$ perpendicular to the trajectory and $0.07m$ along the trajectory. The averaged final navigation error was reduced from $3.24m$ to $0.50m$. More than $6\times$ of the systematic error reduction was demonstrated, indicating feasibility of the compensation method. After systematic error compensation, the error caused by IMU noises became dominant, thus making it possible to improve the overall navigation accuracy by improving IMU performances.

IV. Conclusion

In this study, we identified the residual velocity of the foot during the stance phase and the gyroscope g-sensitivity to be the main factors that cause systematic navigation errors in the ZUPT-aided pedestrian inertial navigation. A compensation result of more than $6\times$ systematic error reduction from $3.24m$ to $0.50m$ during a 100m straight line trajectory was experimentally demonstrated. In this study we greatly reduced the systematic errors in the ZUPT-aided pedestrian inertial navigation, and therefore the errors caused by IMU noises became dominant, making it possible to improve the overall navigation accuracy by improving IMU performances.

References

[1] M. Perlmutter, and L. Robin, "High-performance, low cost inertial MEMS: A market in motion!" *IEEE/ION Position, Location and Navigation Symposium*, Apr. 23-26, 2012, Myrtle Beach, SC, USA.

[2] E. Foxlin, "Pedestrian tracking with shoe-mounted inertial sensors," *IEEE Computer Graphics and Applications*, vol. 25, no. 6, pp. 38-46, 2005.

[3] Y. Wang, A. Chernyshoff, and A. M. Shkel, "Error analysis of ZUPT-aided pedestrian inertial navigation." *IEEE International Conference on Indoor Positioning and Indoor Navigation (IPIN)*, Sep. 24-27, 2018, Nantes, France.

[4] Y. Wang, A. Chernyshoff, and A. M. Shkel, "Study on Estimation Errors in ZUPT-Aided Pedestrian Inertial Navigation Due to IMU Noises," *IEEE Transactions on Aerospace and Electronic Systems*, doi: 10.1109/TAES.2019.2946506.

[5] J. O. Nilsson, I. Skog, and P. Handel, "A note on the limitations of ZUPTs and the implications on sensor error modeling," *IEEE International Conference on Indoor Positioning and Indoor Navigation (IPIN)*, Nov. 13-15, 2012, Sydney, Australia.

[6] Y. Wang, S. Askari, A. M. Shkel, "Study on Mounting Position of IMU for Better Accuracy of ZUPT-Aided Pedestrian Inertial Navigation," *IEEE International Symposium on Inertial Sensors and Systems (INERTIAL)*, Apr. 1-5, 2019, Naples, FL, USA.

[7] Y. Wang and A. M. Shkel, "Adaptive Threshold for Zero-Velocity Detector in ZUPT-Aided Pedestrian Inertial Navigation," *IEEE Sensors Letters*, vol. 3, no. 11, 2019.

[8] H. Martin, P. Groves, and M. Newman, "The Limits of In-Run Calibration of MEMS Inertial Sensors and Sensor Arrays," *NAVIGATION: Journal of The Institute of Navigation*, vol. 63, no. 2, pp. 127-143, 2016.

[9] J. B. Bancroft, and G. Lachapelle, "Estimating MEMS gyroscope g-sensitivity errors in foot mounted navigation," *IEEE Ubiquitous Positioning, Indoor Navigation, and Location Based Service (UPINLBS)*, Oct. 3-4, 2012, Helsinki, Finland.

[10] Y. Wang, D. Vatanparvar, A. Chernyshoff, and A. M. Shkel, "Analytical Closed-Form Estimation of Position Error on ZUPT-Augmented Pedestrian Inertial Navigation." *IEEE Sensors Letters*, vol. 2, no. 4, pp. 1-4, 2018.

[11] Y. Geng, R. Martins, and J. Sousa, "Accuracy analysis of DVL/IMU/magnetometer integrated navigation system using different IMUs in AUV," *IEEE International Conference on Control and Automation (ICCA)*, June 9-11, 2010, Xiamen, China.

[12] Y. Wang, S. Askari, C. S. Jao, and A. M. Shkel, "Directional ranging for enhanced performance of aided pedestrian inertial navigation," *IEEE International Symposium on Inertial Sensors and Systems (INERTIAL)*, Apr. 1-5, 2019, Naples, FL, USA.

[13] K. Abdulrahim, C. Hide, T. Moore, and C. Hill, "Aiding low cost inertial navigation with building heading for pedestrian navigation," *The Journal of Navigation*, vol. 64, no. 2, pp. 219-233, 2011.

[14] I. Skog, J. O. Nilsson, D. Zachariah, and P. Handel, "Fusing the information from two navigation systems using an upper bound on their maximum spatial separation," *IEEE International Conference on Indoor Positioning and Indoor Navigation (IPIN)*, Nov. 13-15, 2012, Sydney, Australia.

[15] Polhemus PATRIOT two-sensor 6-DOF tracker: https://polhemus.com/_assets/img/PATRIOT_brochure.pdf

[16] I. Skog, P. Handel, J.-O. Nilsson, and J. Rantakokko, "Zero-velocity detection - An algorithm evaluation," *IEEE Transactions on Biomedical Engineering*, vol. 57, no. 11, pp. 2657-2666, 2010.

[17] Z. Zhu, and S. Wang, "A Novel Step Length Estimator Based on Foot-Mounted MEMS Sensors," *Sensors*, vol. 18, no. 12, pp. 4447, 2018.

[18] M. Laverne, M. George, D. Lord, A. Kelly, and T. Mukherjee, "Experimental validation of foot to foot range measurements in pedestrian tracking," *ION GNSS Conference*, Sep. 19-23, 2011, Portland, OR, USA.

[19] A. B. Chatfield, *Fundamentals of high accuracy inertial navigation*, American Institute of Aeronautics and Astronautics, 1997, eISBN: 978-1-60086-646-3.